

Equilibrium climate sensitivity estimated by equilibrating climate models

Article

Accepted Version

Rugenstein, M., Bloch-Johnson, J. ORCID: <https://orcid.org/0000-0002-8465-5383>, Gregory, J. ORCID: <https://orcid.org/0000-0003-1296-8644>, Andrews, T., Mauritsen, T., Li, C., Frölicher, T. L., Paynter, D., Danabasoglu, G., Yang, S., Dufresne, J.-L., Cao, L., Schmidt, G. A., Abe-Ouchi, A., Geoffroy, O. and Knutti, R. (2020) Equilibrium climate sensitivity estimated by equilibrating climate models. *Geophysical Research Letters*, 47 (4). e2019GL083898. ISSN 0094-8276 doi: <https://doi.org/10.1029/2019GL083898>
Available at <https://centaur.reading.ac.uk/87462/>

It is advisable to refer to the publisher's version if you intend to cite from the work. See [Guidance on citing](#).

To link to this article DOI: <http://dx.doi.org/10.1029/2019GL083898>

Publisher: American Geophysical Union

All outputs in CentAUR are protected by Intellectual Property Rights law, including copyright law. Copyright and IPR is retained by the creators or other copyright holders. Terms and conditions for use of this material are defined in the [End User Agreement](#).

www.reading.ac.uk/centaur

CentAUR

Central Archive at the University of Reading

Reading's research outputs online

Equilibrium climate sensitivity estimated by equilibrating climate models

Maria Rugenstein^{1,2*}, Jonah Bloch-Johnson³, Jonathan Gregory^{3,4}, Timothy
Andrews⁴, Thorsten Mauritsen⁵, Chao Li², Thomas L. Frölicher^{6,7}, David
Paynter⁸, Gokhan Danabasoglu⁹, Shuting Yang¹⁰, Jean-Louis Dufresne¹¹, Long
Cao¹², Gavin A. Schmidt¹³, Ayako Abe-Ouchi¹⁴, Olivier Geoffroy¹⁵, and Reto
Knutti¹

¹Institute for Atmospheric and Climate Science, ETH Zurich, CH-8092 Zurich, Switzerland

²Max-Planck-Institute for Meteorology, Bundestrasse 53, 20146 Hamburg, Germany

³NCAS, University of Reading, Reading

⁴UK Met Office Hadley Centre, FitzRoy Road, Exeter, EX1 3PB

⁵Stockholm University, SE-106 91 Stockholm, Sweden

⁶Climate and Environmental Physics, Physics Institute, University of Bern, Switzerland

⁷Oeschger Centre for Climate Change Research, University of Bern, Switzerland

⁸Geophysical Fluid Dynamics Laboratory, Princeton, New Jersey, USA

⁹National Center for Atmospheric Research, P.O. Box 3000, Boulder, CO 80307

¹⁰Danish Meteorological Institute, Lyngbyvej 100, DK-2100 Copenhagen, Denmark

¹¹LMD/IPSL, Centre National de la Recherche Scientifique, Sorbonne Université, École Normale
Supérieure, PSL Research University, École Polytechnique, Paris, France

¹²School of Earth Sciences, Zhejiang University, Hang Zhou, Zhejiang Province, 310027, China

¹³NASA Goddard Institute for Space Studies, 2880 Broadway, New York, NY 10025

¹⁴Atmosphere and Ocean Research Institute, The University of Tokyo, Japan

¹⁵Centre National de Recherches Météorologiques, Université de Toulouse, Météo-France, CNRS,
Toulouse, France

Key Points:

- 27 simulations of 15 general circulation models are integrated to near equilibrium
- All models simulate a higher equilibrium warming than predicted by using extrapolation methods
- Tropics and mid-latitudes dominate the change of the feedback parameter on different timescales

*Max-Planck-Institute for Meteorology, Bundestrasse 53, 20146 Hamburg, Germany

Corresponding author: Maria Rugenstein, maria.rugenstein@mpimet.mpg.de

Abstract

The methods to quantify equilibrium climate sensitivity are still debated. We collect millennial-length simulations of coupled climate models and show that the global mean equilibrium warming is higher than those obtained using extrapolation methods from shorter simulations. Specifically, 27 simulations with 15 climate models forced with a range of CO₂ concentrations show a median 17% larger equilibrium warming than estimated from the first 150 years of the simulations. The spatial patterns of radiative feedbacks change continuously, in most regions reducing their tendency to stabilizing the climate. In the equatorial Pacific, however, feedbacks become more stabilizing with time. The global feedback evolution is initially dominated by the tropics, with eventual substantial contributions from the mid-latitudes. Time-dependent feedbacks underscore the need of a measure of climate sensitivity that accounts for the degree of equilibration, so that models, observations, and paleo proxies can be adequately compared and aggregated to estimate future warming.

1 Estimating equilibrium climate sensitivity

The equilibrium climate sensitivity (ECS) is defined as the global- and time-mean, surface air warming once radiative equilibrium is reached in response to doubling the atmospheric CO₂ concentration above pre-industrial levels. It is by far the most commonly and continuously applied concept to assess our understanding of the climate system as simulated in climate models and it is used to compare models, observations, and paleo-proxies (Knutti et al., 2017; Charney et al., 1979; Houghton et al., 1990; Stocker, 2013). Due to the large heat capacity of the oceans, the climate system takes millennia to equilibrate to a forcing, but performing such a long simulation with a climate model is often computationally not feasible. As a result, many modeling studies use extrapolation methods on short, typically 150-year long, simulations to project equilibrium conditions (Taylor et al., 2011; Andrews et al., 2012; Collins et al., 2013; Otto et al., 2013; Lewis & Curry, 2015; Andrews et al., 2015; Forster, 2016; Calel & Stainforth, 2017). These so-called *effective* climate sensitivities (Murphy, 1995; Gregory et al., 2004) are often reported as ECS values (Hargreaves & Annan, 2016; Tian, 2015; Brient & Schneider, 2016; Forster, 2016). Research provides evidence for decadal-to-centennial changes of feedbacks (e.g., Murphy (1995); Senior and Mitchell (2000); Gregory et al. (2004); Winton et al. (2010); Armour et al. (2013); Proistosescu and Huybers (2017); Paynter et al. (2018)) but the behavior on longer timescales has

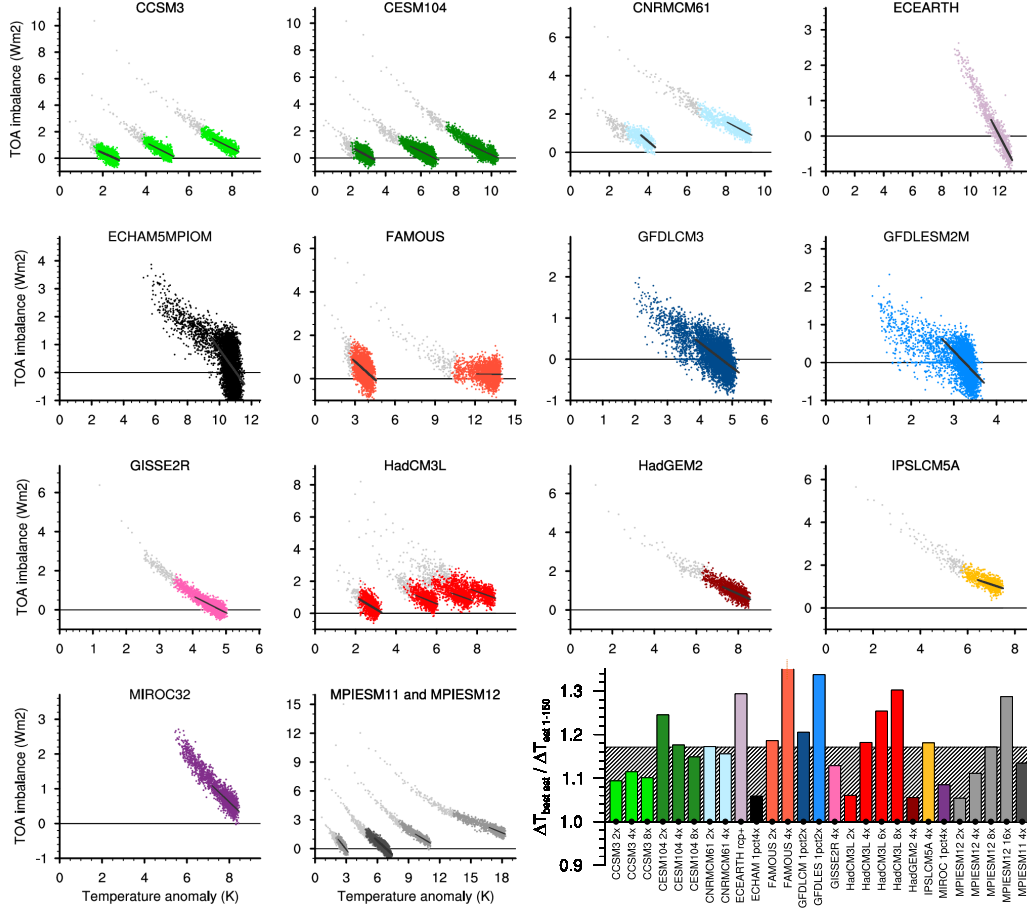


Figure 1. Evolution of global and annual mean top of the atmosphere (TOA) imbalance and surface temperature anomalies (14 small panels). The first 150 years of step forcing simulations are depicted in light gray. For experiments which are not step forcing simulations only the period after stabilizing CO₂ concentrations is shown. The black line shows the linear regression of TOA imbalance and surface warming for the last 15% of warming. The panel on the lower right shows the ratio $\Delta T_{\text{best est}} / \Delta T_{\text{est 1-150}}$, see text for definitions. A dot at the lower end of the bar indicates with 90% confidence that $\Delta T_{\text{best est}}$ and $\Delta T_{\text{est 1-150}}$ obtained by resampling 10,000 times do not overlap. The gray hashed bar in the background is the median of all simulations (1.17). FAMOUS *abrupt4x* ends outside of the depicted range at 1.53. Table 1 specifies the model versions and names, length of simulations, and numerical values for different climate sensitivity estimates.

not been compared among models. Here, we utilize LongRunMIP, a large set of millennia-long coupled general circulations models (GCMs) to estimate the true equilibrium warming, study the centennial-to-millennial behavior of the climate system under elevated radiative forcing, and test extrapolation methods. LongRunMIP is a model intercomparison project (MIP) of opportunity in that its initial contributions were preexisting simulations, without a previously agreed upon protocol. The minimum contribution is a simulation of at least 1000 years with a constant CO₂ forcing level. The collection consists mostly of doubling or quadrupling step forcing simulations (“abrupt2x”, “abrupt4x”, ...) as well as annual increments of 1% CO₂ increases reaching and sustaining doubled or quadrupled concentrations (“1pct2x”, “1pct4x”). Table 1 lists the simulations and models used here, while M. Rugenstein et al. (2019) documents the entire modeling effort and each contribution in detail.

The equilibration of top of the atmosphere (TOA) radiative imbalance and surface temperature anomaly of the simulations are depicted in Fig. 1. Throughout the manuscript, we show anomalies as the difference to the mean of the unforced control simulation with pre-industrial CO₂ concentrations. Light gray dots indicate annual means of the first 150 years of a step forcing simulation, requested by the Coupled Model Intercomparison Project Phase 5 and 6 protocols (CMIP5 and CMIP6; Taylor et al. (2011); Eyring et al. (2016)) and widely used to infer ECS (Andrews et al., 2012; Geoffroy, Saint-Martin, Oliv  , et al., 2013). We refer to this timescale as “decadal to centennial”. Colors indicate the “centennial to millennial” timescale we explore here. The diminishing distances to the reference line at TOA = 0 indicate that most simulations archive near-equilibrium by the end of the simulations. However, even if a simulation has an equilibrated TOA imbalance of near zero, the surface temperature, surface heat fluxes, or ocean temperatures can still show a trend (discussed in M. Rugenstein et al. (2019)).

Throughout the manuscript, we use “ $\Delta T_{[specification]}$ ” for a true or estimated equilibrium warming, for a range of forcing levels not only CO₂ doubling (Table 1). We define the best estimate of equilibrium warming, $\Delta T_{\text{best est}}$, as the temperature-axis intersect of the regression of annual means of TOA imbalance and surface temperature anomaly over the simulations’ final 15% of global mean warming (black lines in Fig. 1). The lower right panel in Fig. 1 illustrates that all simulations eventually warm significantly more (measured by $\Delta T_{\text{best est}}$) than predicted by the most commonly used method to estimate the equilibrium temperature by extrapolating a least-square regression of the first 150 years of the same step forcing simulation (Gregory et al., 2004; Flato et al., 2013), denoted here as “ $\Delta T_{\text{est } 1-150}$ ”.

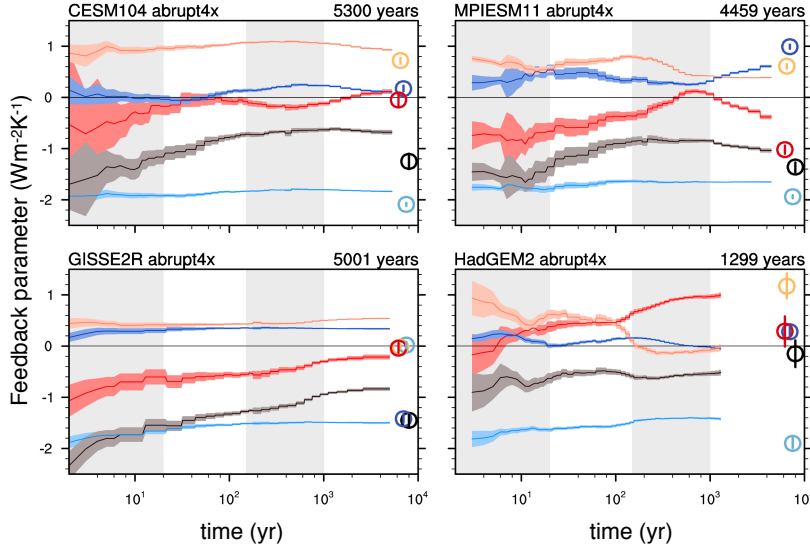
For simulations that have gradual forcings (e.g., *1pct2x*), we use 150 year long step forcing simulations of the same model to calculate $\Delta T_{\text{est } 1-150}$. The median increase of $\Delta T_{\text{best est}}$ over $\Delta T_{\text{est } 1-150}$ is 17% for all simulations and 16% for the subset of CO₂ doubling and quadrupling simulations. While $\Delta T_{\text{est } 1-150}$ implies a constant feedback parameter (the slope of the regression line), other extrapolation methods allow for a time-dependent feedback parameter, but still typically underestimate $\Delta T_{\text{best est}}$: Using years 20-150 in linear regression ($\Delta T_{\text{est } 20-150}$; e.g., Andrews et al. (2015); Armour (2017)) results in a median equilibrium warming estimate which is 7% lower than $\Delta T_{\text{best est}}$, both for all simulations and the subset of CO₂ doubling and quadrupling. The two-layer model including ocean heat uptake efficacy ($\Delta T_{\text{EBM}-\epsilon}$; e.g., Winton et al. (2010); Geoffroy, Saint-Martin, Bellon, et al. (2013)) results in a multi model median equilibrium warming estimate which is 9% lower than $\Delta T_{\text{best est}}$, again both for all simulations and the subset of CO₂ doubling and quadrupling. Both methods are described and illustrated in the supplemental material.

$\Delta T_{\text{best est}}$ of any forcing level can be scaled down to doubling CO₂ levels to estimate equilibrium warming for CO₂ doubling. We do so by assuming that the temperature scales with the forcing level, which depends logarithmically on the CO₂ concentration (Myhre et al., 1998), and assuming no feedback temperature dependence (e.g. Mauritsen et al. (2018) and Rohrschneider et al. (2019), see discussion below). The estimate of equilibrium warming for CO₂ doubling range from 2.42 to 5.83 K (excluding FAMOUS *abrupt4x* at 8.55 K; see Table 1 and Fig. 1). Note that the simulation *abrupt4x* of the model FAMOUS warms anomalously strongly. As this simulation represents a physically possible result, we do not exclude it from the analysis (see more details in SM Section 4). The results are qualitatively the same if $\Delta T_{\text{best est}}$ is defined by regressing over the last 20% instead of 15% of warming or instead time averaging the surface warming toward the end of every simulation without taking the information of the TOA imbalance into account. SM Section 1 discusses different options and choices to determine $\Delta T_{\text{best est}}$.

2 Global feedback evolution

Current extrapolation methods underestimate the equilibrium response because climate feedbacks change with the degree of equilibration (Murphy, 1995; Senior & Mitchell, 2000; Andrews et al., 2015; Knutti & Rugenstein, 2015; M. A. A. Rugenstein, Caldeira, & Knutti, 2016; Armour, 2017; Proistosescu & Huybers, 2017; Paynter et al., 2018). We define the global net TOA feedback as the *local tangent* in temperature-TOA space ($\delta\text{TOA}/\delta T$) com-

a) Time evolution of feedbacks in four models



b) Feedback components for different time periods

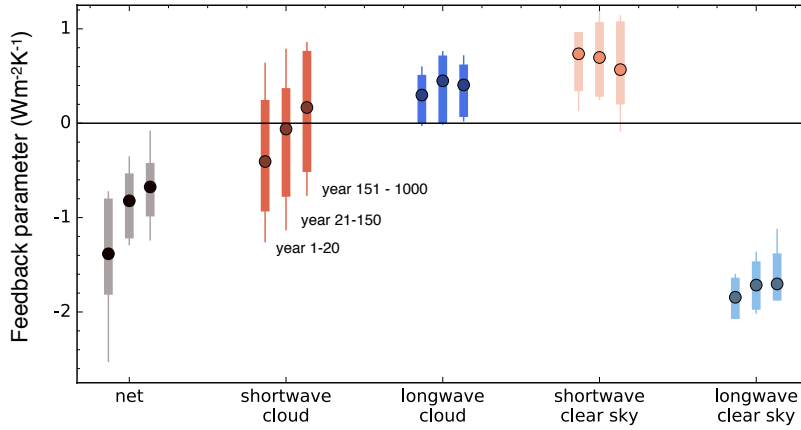


Figure 2. a) Time evolution of global feedbacks in four characteristic models. Net TOA feedback (gray) is the sum of its components: the cloud effects in the shortwave (red) and longwave (blue), and clear sky feedbacks in the shortwave (salmon) and longwave (light blue). Circles at the right of each panel indicate the feedbacks arising from internal variability; shading and vertical lines shows the 2.5-97.5% confidence intervals. Panel titles give the model name and length of the simulation. Time periods of 1-20 years and 150-1000 years are shaded gray. (b) Feedback evolution in the step forcing simulations of CCSM3, CESM104, CNRMCM6, ECHAM5MPIOM, FAMOUS, GISS2R, HadCM3L, HadGEM2, IPSLCM5A, MPIESM11, and MPIESM12, see Table 1 for naming convention. Lines show all simulations, dots represent median values and bars spans all but the two highest and two lowest simulations. SM Fig.4 and 5 show the feedback evolution for all available simulations.

puted by a least square regression of all global and annual means of netTOA imbalance and surface temperature anomaly within a temperature bin, which is moved in steps of 0.1 K throughout the temperature space to obtain the continuous local slope of the point cloud (sketched out in SM Fig. 2a). We decompose the net TOA imbalance into its clear sky and cloud radiative effects (CRE; e.g., Wetherald and Manabe (1988); Soden and Held (2006); Ceppi and Gregory (2017)) in the shortwave and longwave (Fig. 2a). The feedbacks change continuously – not on obviously separable timescales – in some models more at the beginning of the simulations (e.g., CESM104), in some models after 150 years (e.g., GISSER2R) or, in some models, intermittently throughout the simulation (e.g., MPIESM11 or HadGEM2). The shortwave CRE dominates the magnitude and the timing of the net feedback change, and can be counteracted by the longwave CRE. The reduction of the shortwave clear sky feedback associated with ice albedo, lapse rate, and water vapor is a function of temperature and occurs on centennial to millennial timescales. Longwave clear sky changes, when present, contribute to the increase of the sensitivity with equilibration time and temperature. The net feedback parameter can be composed of a subtle balance of different components at any time and the forced signal is not obviously linked to the feedback arising from internal variability, defined by regressing all available annual and global means of TOA imbalance and surface temperature anomalies (relative to the mean) of the control simulations (circles in Fig. 2a; Roe (2009); Brown et al. (2014); Zhou et al. (2015); Colman and Hanson (2017)).

Models which are more sensitive than other models – have feedbacks which are more positive – at the beginning of the simulation are generally also more sensitive towards the end. The model spread in the magnitude of feedbacks does not substantially reduce in time, while the feedback parameter change varies from negligible to an order of magnitude. We quantify the continuous changes across models by considering different time periods, namely years 1-20, 21-150, and 151-1000 (Fig. 2b), in each of which we regress all points. In addition to the increase of the feedback parameter between years 1-20 and 21-150, which has been documented for CMIP5 models (Geoffroy, Saint-Martin, Bellon, et al., 2013; Andrews et al., 2015; Proistosescu & Huybers, 2017; Ceppi & Gregory, 2017), there is a further increase from centennial to millennial timescales.

Previous research has shown that the change in feedbacks over time can come about through a dependence of feedback processes on the increasing temperature (Hansen et al., 1984; Jonko et al., 2013; Caballero & Huber, 2013; Meraner et al., 2013; Bloch-Johnson et al., 2015), due to evolving surface warming patterns and feedback processes (“pattern effect”;

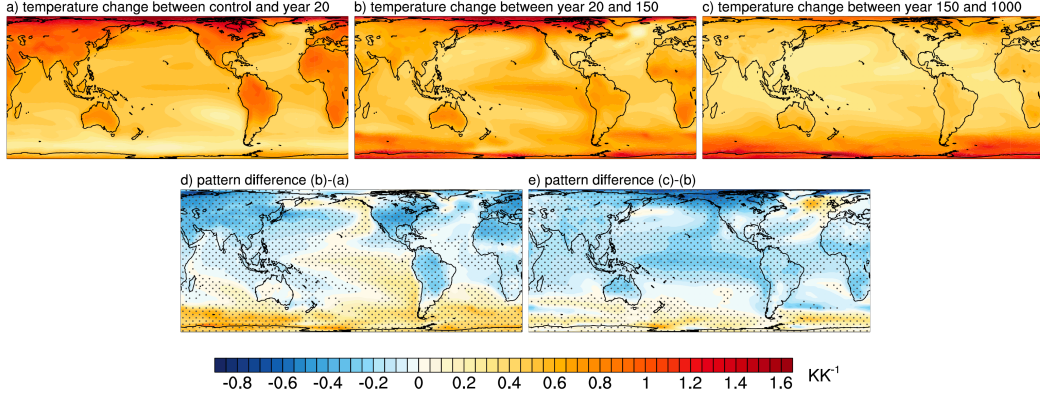


Figure 3. Multi-model mean normalized patterns of surface warming (local warming divided by global warming) between the average of (a) the control simulation and year 15-25, (b) year 15-25 and 140-160, (c) year 140-160 and 800-1000, and their differences (d and e) for the same models and simulations as in Fig. 2b. For models contributing several simulations, these are averaged. Stippling in panel d and e indicates that 9 out of 11 models agree in the sign of change.

Senior and Mitchell (2000); Winton et al. (2010); Armour et al. (2013); M. A. A. Rugenstein, Gregory, et al. (2016); Gregory and Andrews (2016); Haugstad et al. (2017); Paynter et al. (2018)), or both at the same time (Rohrschneider et al., 2019). There is no published method which clearly differentiates between time/pattern and temperature/state dependence and simulations with several forcing levels are needed to disentangle them. The relationship between forcing and CO₂ concentrations is a matter of debate (Etminan et al., 2016) and further complicates the analysis, as time, temperature, and forcing level dependence might compensate to some degree (Gregory et al., 2015). As not all models contributed several forcing levels, we focus in the following on robust pattern changes in surface temperatures and feedbacks, which occur in most or all simulations irrespective of their overall temperature anomaly or forcing level.

3 Pattern evolution of surface warming and feedbacks

The evolution of surface warming patterns during the decadal, centennial, and millennial periods displays a fast establishment of a land-sea warming contrast, Arctic amplification, and the delayed warming over the Southern Ocean that have been studied on annual to centennial timescales (Fig. 3; Senior and Mitchell (2000); Li et al. (2013); Collins et al. (2013); Armour et al. (2016)). Arctic amplification does not change substantially,

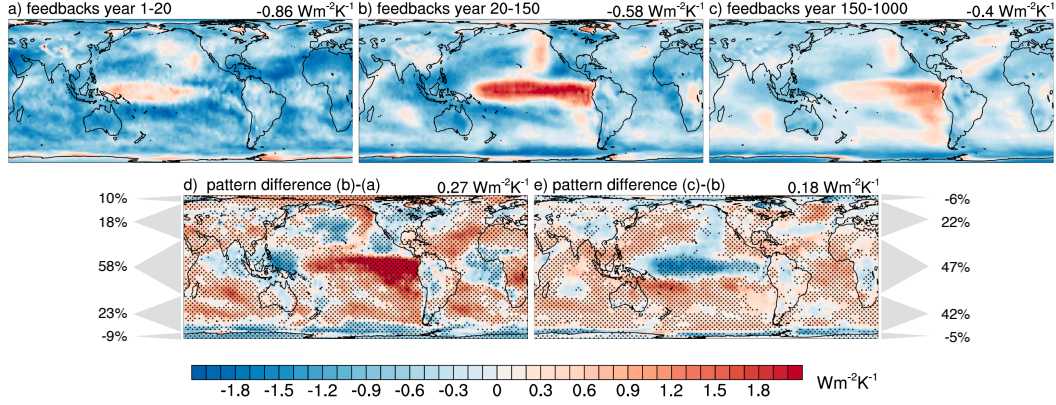


Figure 4. Time evolution of feedback patterns. Model-mean of local contribution to the change in global feedback (local TOA anomaly divided by global warming during the period indicated in the panel titles; see text for definitions) (a–c) and their differences (d,e). The global feedback value is shown in the panel title. Regionally aggregated contributions to the global values are indicated with percent numbers and gray triangles (22°S–22°N, 22°S/N–66°S/N, 66°S/N–90°S/N, representing 40%, 27%, and 4% of the global surface area respectively). Model and simulations selection, weighting, and stippling is the same as in Fig. 3. SM Fig. 6–12 shows all TOA components.

whereas Antarctic amplification strengthens by approximately 50% on centennial to millennial timescales (Salzmann, 2017; M. Rugestein et al., 2019). The warming in the northern North Atlantic reflects the strengthening of the Atlantic meridional overturning circulation, after the initial decline (Stouffer & Manabe, 2003; Li et al., 2013; M. A. A. Rugestein, Sedláček, & Knutti, 2016; Rind et al., 2018; Jansen et al., 2018).

In the Pacific, at all times, the temperatures in absolute terms are higher in the West compared to the East Pacific. The eastern equatorial Pacific warms more than the warm pool in most simulations, a phenomenon reminiscent of the positive phase of the El-Niño-Southern-Oscillation (ENSO) (“ENSO-like warming” (Song & Zhang, 2014; Andrews et al., 2015; Luo et al., 2017; Tierney et al., 2019)). This tendency can last several millennia, but significantly reduces or stops in most simulations after a few hundred years. Similar to the Equatorial east Pacific, the south east Pacific warms more than the warm pool (Zhou et al., 2016; Andrews & Webb, 2018). However, models display a large variance in the timescales of warming in these two regions, i.e. the warm pool can initially warm faster or slower than the south east Pacific. Across the Pacific, the change in surface warming pattern is reminiscent of the Interdecadal Pacific Oscillation (IPO; Fig. 3d). In many models, the reduction

of the Walker circulation coincides with the decadal to centennial ENSO/IPO-like warming pattern, but it does not obviously coincide with surface warming pattern changes on the millennial timescale, indicating that subtropical ocean gyre advection and upwelling play a more prominent role on longer timescales (Knutson & Manabe, 1995; Song & Zhang, 2014; Fedorov et al., 2015; Andrews & Webb, 2018; Luo et al., 2017; Zhou et al., 2017; Kohyama et al., 2017). The mechanisms and spread of model responses in the Pacific are still under investigation.

Feedbacks defined as the local tangent in temperature-TOA space as used in Fig. 2a contain a signal from both the internal variability and the forced response. In order to isolate the forced response, we take the difference of the means at the beginning and end of the time periods discussed above. We call this definition of feedbacks the *finite difference approach*, as it represents a change *across* a time period (SM Fig. 2b). Fig. 4 shows the local contribution to the global net TOA changes (defined as the local change in TOA imbalance divided by the global temperature change.) for the same time periods and models as used in Fig. 3. In the initial years, the atmosphere restores radiative balance through increased radiation to space almost everywhere, except in the western-central Pacific (Fig. 4a), whereas on decadal to centennial timescales, the structure of the feedbacks mirrors the surface temperature evolution and develops a pattern reminiscent of ENSO/IPO (Fig. 4b). The cloud response dominates the pattern change, although for CMIP5 models, changes on decadal and centennial timescales have been attributed to changing lapse rate feedbacks as well (SM Fig. 6-8 and Andrews et al. (2015); Andrews and Webb (2018); Ceppi and Gregory (2017)). For the millennial timescales, our models show that feedbacks become less negative almost everywhere, switching from slightly negative to positive in parts of the Southern Ocean and North Atlantic region, and become less destabilizing in the Tropical Pacific (Fig. 4c). The feedback pattern change from decadal to centennial timescales (Fig. 4d) is reversed in many regions on centennial to millennial timescales (Fig. 4e), particularly in the entire Pacific basin, the Atlantic, and parts of Asia and North America. This “pattern flip” is dominated by longwave CRE (SM Fig. 8) and mirrors, in the Pacific, the reduction in ENSO/IPO-like surface warming patterns discussed for the surface temperature evolution.

Note that the local temperature is not part of the calculation of the local contribution in feedback changes. Due to the far-field effects of local feedbacks (e.g., Rose et al. (2014); Kang and Xie (2014); M. A. A. Rugenstein, Caldeira, and Knutti (2016); Zhou et al. (2016, 2017); Ceppi and Gregory (2017); Liu et al. (2018); Dong et al. (2019)), the relation between

the local feedback contribution (Fig. 4) and the local temperatures (Fig. 3) is not straightforward. There is strong correspondence between changes of TOA fluxes and temperature patterns in the Pacific on decadal to millennial timescales: Stronger (weaker) local warming coincides with a more positive (negative) local feedback contribution. However, there is no clear correspondence directly after the application of the forcing, or over land and the Southern Ocean through time. SM Fig. 13 and 14 show overlays of Fig. 3 and 4 for a better comparison. A local correspondence does not necessarily indicate a strong local feedback (i.e. local TOA divided by local surface temperature change), as both the local TOA and the surface in one region could be forced by another region. A closer investigation of local and far-field influence of feedbacks is under investigation (Bloch-Johnson et al., in revision).

Although the spatial patterns of changing temperature and radiative feedbacks vary among models, the large scale features discussed here occur robustly across most models and forcing levels, and also occur in the *1pct2x* and *1pct4x* simulations, which are not included in the figures.

4 Regions accounting for changing global feedbacks

We quantify the contribution of the tropics, extra-tropics, and polar regions to the global feedback change (Fig. 4d,e) by adding up all feedback contributions of the respective areas indicated by the gray triangles and expressing them as percentages of the total. We note that the total is the global feedback parameter, i.e., the slope of the point clouds in Fig. 1 which is indicated on the top right of each panel. These percentages reflect the role played by TOA fluxes in each region, which is not the same as the role played by surface warming in each region, as noted above. Whereas the tropics account for the bulk of the change (58% on decadal to centennial and 47% on centennial to millennial timescales), the mid-latitudes become more important with time (Northern and Southern Hemisphere combined for 41% on decadal to centennial and for 66% on centennial to millennial timescales). The high latitudes, dominated by the shortwave clear sky feedback (SM Fig. 12), play only a minor role in influencing the global response at all timescales. The regional accounting of global feedback changes permits us to test competing explanations regarding the spatial feedback pattern by placing them in a common temporal framework. Primary regions controlling the global feedback evolution have been suggested to be the Southern Hemisphere mid to high latitudes (Senior & Mitchell, 2000), the Northern Hemisphere subpolar regions (Rose & Rayborn, 2016; Trossman et al., 2016), and the Tropics (Jonko et al., 2013; Mer-

aner et al., 2013; Block & Mauritsen, 2013; Andrews et al., 2015; Ceppi & Gregory, 2019), especially in the Pacific (Andrews & Webb, 2018; Ceppi & Gregory, 2017).

The simulations robustly shows a delayed warming in the Southern Hemisphere relative to the Northern Hemisphere throughout the millennia-long integrations, which correlates with the time evolution of net TOA and shortwave CRE (not shown). This behavior lends support to the hypothesis of Senior and Mitchell (2000) who propose that feedbacks change through time due to the slow warming rates of the Southern Ocean relative to the upper atmospheric levels. This reduced lapse rate increases atmospheric static stability (and thus, the shortwave cloud response) in the transient part of the simulation, but decreasingly less so towards equilibrium.

The extra-tropical cloud response in the model-mean is non-negligible in the Southern Ocean and North Atlantic on decadal to centennial timescales, as proposed by Rose and Rencurrel (2016) and Trossman et al. (2016). However, it comes to dominate the global response only on centennial to millennial timescales and when both hemispheres are considered.

We find that the longwave clear sky feedback does moderately increase in many models as the temperature or the forcing level increases, mainly in the tropics and Northern Hemisphere mid-latitudes (Fig. 2a, SM Fig. 4, SM Fig. 5). This is in accordance with the proposed argument that the tropics govern the global feedback evolution because the water vapor feedback increases with warming (Jonko et al., 2013; Meraner et al., 2013; Block & Mauritsen, 2013; Andrews et al., 2015), possibly following the rising tropical tropopause (Meraner et al., 2013; Mauritsen et al., 2018).

Recent work has focused on the relative influence of the Pacific, specifically the relative influence of temperatures of the warm pool versus compared to other regions. Feedbacks in regions of atmospheric deep convections have a far-field and global effect, while feedbacks in regions of atmospheric subsidence have only a local or regional influence (Barsugli & Sardeshmukh, 2002; Zhou et al., 2017; Andrews & Webb, 2018; Ceppi & Gregory, 2019; Dong et al., 2019). With the available fields in the LongRunMIP archive, we cannot quantify the relative importance of water vapor and lapse rate feedbacks. However, the short and longwave cloud response (SM Fig. 6–8) in the models qualitatively agree with the proposed change of tropospheric stability patterns on decadal to centennial timescales (Andrews & Webb, 2018; Ceppi & Gregory, 2017), especially in the Pacific region. In contrast, on cen-

nial to millennial timescales, the tropical Pacific response becomes less important compared to the mid-latitudes and the net tropical CRE does not change anymore (SM Fig. 6).

5 Implications

We demonstrate that the evolution of the global feedback response is dominated by the mid-latitudes on centennial to millennial and the tropics on decadal to centennial timescales. The global net feedback change is a result of a subtle balance of different regions and different TOA components at all times; even more so in single simulations than in the model mean shown here. This motivates process-based feedback studies in individual models as well as multi-model ensembles to draw robust conclusions and increase physical understanding of processes. To relate the timescales and model behavior to the observational record and paleo proxies a better understanding of a) the atmospheric versus oceanic drivers of surface temperature patterns in both, the coupled climate models and the real world and b) the local and far field interactions of tropospheric stability, clouds, and surface temperatures need to be achieved. Note that climate models have typical and persistent biases in regions we identify as important, mainly the Equatorial Pacific, Southern Ocean and ocean upwelling regions. The pattern effect of the real world might act on timescales which are different than the ones of the climate models.

Our results show that radiative feedbacks, usually called “fast”, act continuously less stabilizing on the climate system as the models approach equilibrium. As a result, the equilibrium warming is higher than estimated with common extrapolation methods from short simulations for all models and simulations in the LongRunMIP archive. ECS has been historically used as a model characterization (Charney et al., 1979), but some studies propose that it is not the most adequate measure for estimating changes expected over the next decades and until the end of the century (e.g., Otto et al. (2013); Shiogama et al. (2016); Knutti et al. (2017)). Alternative climate sensitivity measures are the effective climate sensitivity computed on different timescales, the transient climate response to gradually increasing CO₂ (TCR), or the transient climate response to cumulative carbon emissions (e.g., Allen and Frame (2007); Millar et al. (2015); Gregory et al. (2015); Grose et al. (2018)). Beyond not being an accurate indicator of the equilibrium response, these alternative climate sensitivity measures capture the models in different degrees of equilibration. We show that it is an open question how different measures of sensitivity relate to each other. A recent study shows that $\Delta T_{\text{est } 1-150}$ correlates better than TCR with end-of-21st-century warming

across model (Grose et al. (2018), see also Gregory et al. (2015)). Thus, we underscore the need of comparing models, observations, and paleo proxies on well-defined measures of climate sensitivity, which ensure they are in the same state of equilibration.

Acknowledgments

Fields shown in this paper can be accessed on <https://data.iac.ethz.ch/longrunmip/GRL/>. See www.longrunmip.org and M. Rugenstein et al. (2019) for more details on each simulation and available variables, not shown here.

We thank Urs Beyerle, Erich Fischer, Jeremy Rugenstein, Levi Silvers, and Martin Stolpe for technical help and comments on the manuscript.

MR is funded by the Alexander von Humboldt Foundation. NCAR is a major facility sponsored by the U.S. National Science Foundation under Cooperative Agreement 1852977. TA was supported by the Joint UK BEIS/Defra Met Office Hadley Centre Climate Programme (GA01101). TLF acknowledges support from the Swiss National Science Foundation under Grant PP00P2_170687, from the European Union's Horizon 2020 research and innovation program under grant agreement no. 821003 (CCiCC) CL was supported through the Clusters of Excellence CliSAP (EXC177) and CLICCS (EXC2037), University Hamburg, funded through the German Research Foundation (DFG). SY was partly supported by European Research Council under the European Community's Seventh Framework Programme (FP7/20072013)/ERC grant agreement 610055 as part of the ice2ice project.

References

- Allen, M. R., & Frame, D. J. (2007). Call off the quest. *Science*, *318*(5850), 582-583. Retrieved from <http://www.sciencemag.org/content/318/5850/582.short> doi: 10.1126/science.1149988
- Andrews, T., Gregory, J. M., & Webb, M. J. (2015). The Dependence of Radiative Forcing and Feedback on Evolving Patterns of Surface Temperature Change in Climate Models. *Journal of Climate*, *28*(4), 1630-1648. Retrieved from <http://dx.doi.org/10.1175/JCLI-D-14-00545.1>
- Andrews, T., Gregory, J. M., Webb, M. J., & Taylor, K. E. (2012). Forcing, feedbacks and climate sensitivity in CMIP5 coupled atmosphere-ocean climate models. *Geophysical Research Letters*, *39*(9). Retrieved from <http://dx.doi.org/10.1029/2012GL051607>
- Andrews, T., & Webb, M. J. (2018). The Dependence of Global Cloud and Lapser Rate Feedbacks on the Spatial Structure of Tropical Pacific Warming. *Journal of Climate*, *31*(2), 641-654. Retrieved from <https://doi.org/10.1175/JCLI-D-17-0087.1>
- Armour, K. C. (2017). Energy budget constraints on climate sensitivity in light of inconstant climate feedbacks. *Nature Climate Change*, *7*, 331 EP -. Retrieved from <http://dx.doi.org/10.1038/nclimate3278>
- Armour, K. C., Bitz, C. M., & Roe, G. H. (2013). Time-Varying Climate Sensitivity from Regional Feedbacks. *Journal of Climate*, *26*(13), 4518-4534. Retrieved from <http://dx.doi.org/10.1175/JCLI-D-12-00544.1>
- Armour, K. C., Marshall, J., Scott, J. R., Donohoe, A., & Newsom, E. R. (2016). Southern ocean warming delayed by circumpolar upwelling and equatorward transport. *Nature Geosci*, *9*(7), 549-554. Retrieved from <http://dx.doi.org/10.1038/ngeo2731>
- Barsugli, J. J., & Sardeshmukh, P. D. (2002). Global atmospheric sensitivity to tropical sst anomalies throughout the indo-pacific basin. *Journal of Climate*, *15*(23), 3427-3442. Retrieved from [https://doi.org/10.1175/1520-0442\(2002\)015<3427:GASTTS>2.0.CO;2](https://doi.org/10.1175/1520-0442(2002)015<3427:GASTTS>2.0.CO;2)
- Bloch-Johnson, J., Pierrehumbert, R. T., & Abbot, D. S. (2015). Feedback temperature dependence determines the risk of high warming. *Geophysical Research Letters*, *42*(12), 4973- 4980. Retrieved from <http://dx.doi.org/10.1002/2015GL064240> (2015GL064240)
- Bloch-Johnson, J., Rugenstein, M., & Abbot, D. S. (in revision). Spatial radiative feedbacks from interannual variability using multiple regression. *Journal of Climate*.

- Block, K., & Mauritsen, T. (2013). Forcing and feedback in the MPI-ESM-LR coupled model under abruptly quadrupled CO₂. *Journal of Advances in Modeling Earth Systems*, 5(4), 676–691. Retrieved from <http://dx.doi.org/10.1002/jame.20041>
- Brient, F., & Schneider, T. (2016). Constraints on Climate Sensitivity from Space-Based Measurements of Low-Cloud Reflection. *Journal of Climate*, 29(16), 5821–5835. Retrieved from <https://doi.org/10.1175/JCLI-D-15-0897.1>
- Brown, P. T., Li, W., Li, L., & Ming, Y. (2014). Top-of-atmosphere radiative contribution to unforced decadal global temperature variability in climate models. *Geophysical Research Letters*, 41(14), 5175–5183. Retrieved from <http://dx.doi.org/10.1002/2014GL060625>
- Caballero, R., & Huber, M. (2013). State-dependent climate sensitivity in past warm climates and its implications for future climate projections. *Proceedings of the National Academy of Sciences of the United States of America*, 110(35), 14162–14167. Retrieved from <http://www.ncbi.nlm.nih.gov/pmc/articles/PMC3761583/>
- Calel, R., & Stainforth, D. A. (2017). On the Physics of Three Integrated Assessment Models. *Bulletin of the American Meteorological Society*, 98(6), 1199–1216. Retrieved from <https://doi.org/10.1175/BAMS-D-16-0034.1>
- Ceppi, P., & Gregory, J. M. (2017). Relationship of tropospheric stability to climate sensitivity and earth’s observed radiation budget. *Proceedings of the National Academy of Sciences*, 114(50), 13126–13131. Retrieved from <https://www.pnas.org/content/114/50/13126>
- Ceppi, P., & Gregory, J. M. (2019). A refined model for the Earth’s global energy balance. *Climate Dynamics*. Retrieved from <https://doi.org/10.1007/s00382-019-04825-x>
- Charney, J., Arakawa, A., Baker, D., Bolin, B., Dickinson, R. E., Goody, R., ... Wunsch, C. (1979). *Carbon Dioxide and Climate: A Scientific Assessment* (Tech. Rep.). Washington, DC.: National Academy of Science.
- Collins, M., Knutti, R., Arblaster, J. M., Dufresne, J.-L., Fichet, T., Friedlingstein, P., ... Wehner, M. F. (2013). Long-term Climate Change: Projections, Commitments and Irreversibility. In T. Stocker et al. (Eds.), Cambridge University Press, Cambridge, United Kingdom and New York, NY, USA.
- Colman, R., & Hanson, L. (2017). On the relative strength of radiative feedbacks under climate variability and change. *Climate Dynamics*, 49(5), 2115–2129. Retrieved from

- 407 <https://doi.org/10.1007/s00382-016-3441-8>
- 408 Dong, Y., Proistosescu, C., Armour, K. C., & Battisti, D. S. (2019). Attributing Historical
409 and Future Evolution of Radiative Feedbacks to Regional Warming Patterns using
410 a Green's Function Approach: The Preeminence of the Western Pacific. *Journal of*
411 *Climate*, 0(0), null. Retrieved from <https://doi.org/10.1175/JCLI-D-18-0843.1>
- 412 Etminan, M., Myhre, G., Highwood, E. J., & Shine, K. P. (2016). Radiative forcing
413 of carbon dioxide, methane, and nitrous oxide: A significant revision of the methane
414 radiative forcing. *Geophysical Research Letters*, 43(24), 12,614–12,623. Retrieved from
415 <https://agupubs.onlinelibrary.wiley.com/doi/abs/10.1002/2016GL071930>
- 416 Eyring, V., Bony, S., Meehl, G. A., Senior, C. A., Stevens, B., Stouffer, R. J., & Taylor, K. E.
417 (2016). Overview of the Coupled Model Intercomparison Project Phase 6 (CMIP6)
418 experimental design and organization. *Geoscientific Model Development*, 9(5), 1937–
419 1958. Retrieved from <https://www.geosci-model-dev.net/9/1937/2016/>
- 420 Fedorov, A. V., Burls, N. J., Lawrence, K. T., & Peterson, L. C. (2015). Tightly linked
421 zonal and meridional sea surface temperature gradients over the past five million
422 years. *Nature Geoscience*, 8, 975 EP -. Retrieved from [https://doi.org/10.1038/](https://doi.org/10.1038/ngeo2577)
423 [ngeo2577](https://doi.org/10.1038/ngeo2577)
- 424 Flato, G., Marotzke, J., Abiodun, B., Braconnot, P., Chou, S., Collins, W., ... Rum-
425 mukainen, M. (2013). Evaluation of Climate Models. In T. Stocker et al. (Eds.),
426 Cambridge University Press, Cambridge, United Kingdom and New York, NY, USA.
- 427 Forster, P. M. (2016). Inference of climate sensitivity from analysis of earth's energy
428 budget. *Annual Review of Earth and Planetary Sciences*, 44(1), 85–106. Retrieved
429 from <http://dx.doi.org/10.1146/annurev-earth-060614-105156>
- 430 Geoffroy, O., Saint-Martin, D., Bellon, G., Voldoire, A., Olivié, D., & Tytéca, S. (2013).
431 Transient Climate Response in a Two-Layer Energy-Balance Model. Part II: Rep-
432 resentation of the Efficacy of Deep-Ocean Heat Uptake and Validation for CMIP5
433 AOGCMs. *Journal of Climate*, 26(6), 1859–1876. Retrieved from [http://dx.doi](http://dx.doi.org/10.1175/JCLI-D-12-00196.1)
434 [.org/10.1175/JCLI-D-12-00196.1](http://dx.doi.org/10.1175/JCLI-D-12-00196.1)
- 435 Geoffroy, O., Saint-Martin, D., Olivié, D. J. L., Voldoire, A., Bellon, G., & Tytéca, S.
436 (2013). Transient Climate Response in a Two-Layer Energy-Balance Model. Part I:
437 Analytical Solution and Parameter Calibration Using CMIP5 AOGCM Experiments.
438 *Journal of Climate*, 26(6), 1841–1857. Retrieved from [http://dx.doi.org/10.1175/](http://dx.doi.org/10.1175/JCLI-D-12-00195.1)
439 [JCLI-D-12-00195.1](http://dx.doi.org/10.1175/JCLI-D-12-00195.1)

- 440 Good, P., Andrews, T., Chadwick, R., Dufresne, J.-L., Gregory, J. M., Lowe, J. A., ...
 441 Shiogama, H. (2016). nonlinMIP contribution to CMIP6: model intercomparison
 442 project for non-linear mechanisms: physical basis, experimental design and analysis
 443 principles (v1.0). *Geoscientific Model Development*, 9(11), 4019–4028. Retrieved from
 444 <https://www.geosci-model-dev.net/9/4019/2016/>
- 445 Good, P., Lowe, J. A., Andrews, T., Wiltshire, A., Chadwick, R., Ridley, J. K., ... Shi-
 446 iogama, H. (2015, 02). Nonlinear regional warming with increasing co2 concentrations.
 447 *Nature Clim. Change*, 5(2), 138–142.
- 448 Gregory, J. M., & Andrews, T. (2016). Variation in climate sensitivity and feedback param-
 449 eters during the historical period. *Geophysical Research Letters*, 43(8), 3911–3920.
 450 Retrieved from <http://dx.doi.org/10.1002/2016GL068406>
- 451 Gregory, J. M., Andrews, T., & Good, P. (2015). The inconstancy of the transient
 452 climate response parameter under increasing CO₂. *Philosophical Transactions of*
 453 *the Royal Society of London A: Mathematical, Physical and Engineering Sciences*,
 454 373(2054). Retrieved from [http://rsta.royalsocietypublishing.org/content/](http://rsta.royalsocietypublishing.org/content/373/2054/20140417)
 455 [373/2054/20140417](http://rsta.royalsocietypublishing.org/content/373/2054/20140417)
- 456 Gregory, J. M., Ingram, W. J., Palmer, M. A., Jones, G. S., Stott, P. A., Thorpe, R. B., ...
 457 Williams, K. D. (2004). A new method for diagnosing radiative forcing and climate
 458 sensitivity. *Geophysical Research Letters*, 31(3). Retrieved from [http://dx.doi.org/](http://dx.doi.org/10.1029/2003GL018747)
 459 [10.1029/2003GL018747](http://dx.doi.org/10.1029/2003GL018747)
- 460 Grose, M. R., Gregory, J., Colman, R., & Andrews, T. (2018). What Climate Sensitivity
 461 Index Is Most Useful for Projections? *Geophysical Research Letters*, 45(3), 1559–1566.
 462 Retrieved from <http://dx.doi.org/10.1002/2017GL075742>
- 463 Hansen, J., Lacis, A., Rind, D., Russel, G., Stone, P., Fung, I., ... Lerner, J. (1984).
 464 Analysis of feedback mechanisms. In: Climate processes and climate sensitivity. In
 465 J. Hansen & T. Takahashi (Eds.), *Climate sensitivity: Analysis of feedback mecha-*
 466 *nisms* (Vol. 5, pp. 130–163). American Geophysical Union, Washington, DC: AGU
 467 Geophysical Monograph 29, Maurice Ewing.
- 468 Hargreaves, J. C., & Annan, J. D. (2016). Could the pliocene constrain the equilibrium
 469 climate sensitivity? *Climate of the Past*, 12(8), 1591–1599. Retrieved from [http://](http://www.clim-past.net/12/1591/2016/)
 470 www.clim-past.net/12/1591/2016/
- 471 Haugstad, A. D., Armour, K. C., Battisti, D. S., & Rose, B. E. J. (2017). Relative roles
 472 of surface temperature and climate forcing patterns in the inconstancy of radiative

- 473 feedbacks. *Geophysical Research Letters*, 44(14), 7455–7463. Retrieved from [https://](https://agupubs.onlinelibrary.wiley.com/doi/abs/10.1002/2017GL074372)
 474 agupubs.onlinelibrary.wiley.com/doi/abs/10.1002/2017GL074372
- 475 Houghton, J., Jenkins, G. J., & Ephraums, J. J. (1990). Report prepared for Intergovern-
 476 mental Panel on Climate Change by Working Group I. In *Climate Change: The IPCC*
 477 *Scientific Assessment* (p. 410). Cambridge University Press.
- 478 Jansen, M. F., Nadeau, L.-P., & Merlis, T. M. (2018). Transient versus Equilibrium Response
 479 of the Ocean’s Overturning Circulation to Warming. *Journal of Climate*, 31(13), 5147–
 480 5163. Retrieved from <https://doi.org/10.1175/JCLI-D-17-0797.1>
- 481 Jonko, A. K., Shell, K. M., Sanderson, B. M., & Danabasoglu, G. (2013). Climate Feedbacks
 482 in CCSM3 under Changing CO2 Forcing. Part II: Variation of Climate Feedbacks
 483 and Sensitivity with Forcing. *Journal of Climate*, 26(9), 2784–2795. Retrieved from
 484 <http://dx.doi.org/10.1175/JCLI-D-12-00479.1>
- 485 Kang, S. M., & Xie, S.-P. (2014). Dependence of Climate Response on Meridional Structure
 486 of External Thermal Forcing. *Journal of Climate*, 27(14), 5593–5600. Retrieved from
 487 <http://dx.doi.org/10.1175/JCLI-D-13-00622.1>
- 488 Knutson, T. R., & Manabe, S. (1995). Time-Mean Response over the Tropical Pacific
 489 to Increased CO₂ in a Coupled Ocean-Atmosphere Model. *Journal of Climate*, 8(9),
 490 2181–2199. Retrieved from [https://doi.org/10.1175/1520-0442\(1995\)008<2181:](https://doi.org/10.1175/1520-0442(1995)008<2181:TMROTT>2.0.CO;2)
 491 [TMROTT>2.0.CO;2](https://doi.org/10.1175/1520-0442(1995)008<2181:TMROTT>2.0.CO;2)
- 492 Knutti, R., & Rugenstein, M. A. A. (2015). Feedbacks, climate sensitivity and the limits of
 493 linear models. *Philosophical Transactions of the Royal Society of London A: Mathe-*
 494 *matical, Physical and Engineering Sciences*, 373(2054). doi: 10.1098/rsta.2015.0146
- 495 Knutti, R., Rugenstein, M. A. A., & Hegerl, G. C. (2017). Beyond equilibrium climate
 496 sensitivity. *Nature Geoscience*, 10, 727 EP -. Retrieved from [http://dx.doi.org/](http://dx.doi.org/10.1038/ngeo3017)
 497 [10.1038/ngeo3017](http://dx.doi.org/10.1038/ngeo3017)
- 498 Kohyama, T., Hartmann, D. L., & Battisti, D. S. (2017). La Nina-like Mean-State Response
 499 to Global Warming and Potential Oceanic Roles. *Journal of Climate*, 30(11), 4207–
 500 4225. Retrieved from <https://doi.org/10.1175/JCLI-D-16-0441.1>
- 501 Lewis, N., & Curry, J. A. (2015). The implications for climate sensitivity of AR5 forcing
 502 and heat uptake estimates. *Climate Dynamics*, 45(3), 1009–1023. Retrieved from
 503 <http://dx.doi.org/10.1007/s00382-014-2342-y>
- 504 Li, C., Storch, J.-S., & Marotzke, J. (2013). Deep-ocean heat uptake and equilibrium
 505 climate response. *Climate Dynamics*, 40(5-6), 1071–1086. Retrieved from <http://>

- 506 [dx.doi.org/10.1007/s00382-012-1350-z](https://doi.org/10.1007/s00382-012-1350-z)
- 507 Liu, F., Lu, J., Garuba, O. A., Huang, Y., Leung, L. R., Harrop, B. E., & Luo, Y. (2018).
 508 Sensitivity of Surface Temperature to Oceanic Forcing via q-Flux Green's Function
 509 Experiments. Part II: Feedback Decomposition and Polar Amplification. *Journal of*
 510 *Climate*, *31*(17), 6745-6761. Retrieved from <https://doi.org/10.1175/JCLI-D-18>
 511 -0042.1
- 512 Luo, Y., Lu, J., Liu, F., & Garuba, O. (2017). The Role of Ocean Dynamical Thermostat in
 513 Delaying the El Niño-Like Response over the Equatorial Pacific to Climate Warming.
 514 *Journal of Climate*, *30*(8), 2811-2827. Retrieved from <https://doi.org/10.1175/>
 515 JCLI-D-16-0454.1
- 516 Mauritsen, T., Bader, J., Becker, T., Behrens, J., Bittner, M., Brokopf, R., ... Roeck-
 517 ner, E. (2018). Developments in the mpi-m earth system model version 1.2 (mpi-
 518 esm 1.2) and its response to increasing co2. *Journal of Advances in Modeling Earth*
 519 *Systems*, *0*(ja). Retrieved from [https://agupubs.onlinelibrary.wiley.com/doi/](https://agupubs.onlinelibrary.wiley.com/doi/abs/10.1029/2018MS001400)
 520 [abs/10.1029/2018MS001400](https://agupubs.onlinelibrary.wiley.com/doi/abs/10.1029/2018MS001400)
- 521 Meraner, K., Mauritsen, T., & Voigt, A. (2013). Robust increase in equilibrium climate
 522 sensitivity under global warming. *Geophysical Research Letters*, *40*(22), 5944-5948.
 523 Retrieved from <http://dx.doi.org/10.1002/2013GL058118>
- 524 Millar, R. J., Otto, A., Forster, P. M., Lowe, J. A., Ingram, W. J., & Allen, M. R. (2015).
 525 Model structure in observational constraints on transient climate response. *Climatic*
 526 *Change*, *131*(2), 199-211. Retrieved from <https://doi.org/10.1007/s10584-015>
 527 -1384-4
- 528 Murphy, J. M. (1995). Transient Response of the Hadley Centre Coupled Ocean-Atmosphere
 529 Model to Increasing Carbon Dioxide. Part 1: Control Climate and Flux Adjustment.
 530 *Journal of Climate*, *8*(1), 36-56. Retrieved from <http://dx.doi.org/10.1175/1520>
 531 -0442(1995)008<0036:TROTHC>2.0.CO;2
- 532 Myhre, G., Highwood, E. J., Shine, K. P., & Stordal, F. (1998). New estimates of radiative
 533 forcing due to well mixed greenhouse gases. *Geophysical Research Letters*, *25*(14),
 534 2715-2718. Retrieved from [https://agupubs.onlinelibrary.wiley.com/doi/abs/](https://agupubs.onlinelibrary.wiley.com/doi/abs/10.1029/98GL01908)
 535 [10.1029/98GL01908](https://agupubs.onlinelibrary.wiley.com/doi/abs/10.1029/98GL01908)
- 536 Otto, A., Otto, F. E. L., Boucher, O., Church, J., Hegerl, G., Forster, P. M., ... Allen,
 537 M. R. (2013). Energy budget constraints on climate response. *Nature Geosci*, *6*(6),
 538 415-416. Retrieved from <http://dx.doi.org/10.1038/ngeo1836>

- Paynter, D., Frölicher, T. L., Horowitz, L. W., & Silvers, L. G. (2018). Equilibrium Climate Sensitivity Obtained From Multimillennial Runs of Two GFDL Climate Models. *Journal of Geophysical Research: Atmospheres*, 123(4), 1921-1941. Retrieved from <https://agupubs.onlinelibrary.wiley.com/doi/abs/10.1002/2017JD027885>
- Proistosescu, C., & Huybers, P. J. (2017). Slow climate mode reconciles historical and model-based estimates of climate sensitivity. *Science Advances*, 3(7). Retrieved from <http://advances.sciencemag.org/content/3/7/e1602821>
- Rind, D., Schmidt, G. A., Jonas, J., Miller, R., Nazarenko, L., Kelley, M., & Romanski, J. (2018). Multicentury Instability of the Atlantic Meridional Circulation in Rapid Warming Simulations With GISS ModelE2. *Journal of Geophysical Research: Atmospheres*, 123(12), 6331-6355. Retrieved from <https://agupubs.onlinelibrary.wiley.com/doi/abs/10.1029/2017JD027149>
- Roe, G. (2009). Feedbacks, timescales, and seeing red. *Annual Review of Earth and Planetary Sciences*, 37(1), 93-115. Retrieved from <http://dx.doi.org/10.1146/annurev.earth.061008.134734>
- Rohrschneider, T., Stevens, B., & Mauritsen, T. (2019, 02). On simple representations of the climate response to external radiative forcing. *Climate Dynamics*. doi: 10.1007/s00382-019-04686-4
- Rose, B. E. J., Armour, K. C., Battisti, D. S., Feldl, N., & Koll, D. D. B. (2014). The dependence of transient climate sensitivity and radiative feedbacks on the spatial pattern of ocean heat uptake. *Geophysical Research Letters*, 41(3), 1071–1078. Retrieved from <http://dx.doi.org/10.1002/2013GL058955>
- Rose, B. E. J., & Rayborn, L. (2016). The Effects of Ocean Heat Uptake on Transient Climate Sensitivity. *Current Climate Change Reports*, 1–12. Retrieved from <http://dx.doi.org/10.1007/s40641-016-0048-4>
- Rose, B. E. J., & Rencurrel, M. C. (2016). The Vertical Structure of Tropospheric Water Vapor: Comparing Radiative and Ocean-Driven Climate Changes. *Journal of Climate*, 29(11), 4251-4268. Retrieved from <http://dx.doi.org/10.1175/JCLI-D-15-0482.1>
- Rugenstein, M., Bloch-Johnson, J., Abe-Ouchi, A., Andrews, T., Beyerle, U., Cao, L., ... Yang, S. (2019). LongRunMIP – motivation and design for a large collection of millennial-length GCM simulations. *Bulletin of the American Meteorological Society*, 0(0), null. Retrieved from <https://doi.org/10.1175/BAMS-D-19-0068.1>

- 572 Rugenstein, M. A. A., Caldeira, K., & Knutti, R. (2016). Dependence of global radiative
573 feedbacks on evolving patterns of surface heat fluxes. *Geophysical Research Letters*,
574 *43*(18), 9877–9885. Retrieved from <http://dx.doi.org/10.1002/2016GL070907>
- 575 Rugenstein, M. A. A., Gregory, J. M., Schaller, N., Sedláček, J., & Knutti, R. (2016). Mul-
576 tiannual Ocean–Atmosphere Adjustments to Radiative Forcing. *Journal of Climate*,
577 *29*(15), 5643–5659. Retrieved from <http://dx.doi.org/10.1175/JCLI-D-16-0312>
578 .1
- 579 Rugenstein, M. A. A., Sedláček, J., & Knutti, R. (2016). Nonlinearities in patterns of
580 long-term ocean warming. *Geophysical Research Letters*, *43*(7), 3380–3388. Retrieved
581 from <http://dx.doi.org/10.1002/2016GL068041>
- 582 Salzmann, M. (2017). The polar amplification asymmetry: role of Antarctic surface height.
583 *Earth System Dynamics*, *8*(2), 323–336. Retrieved from <https://www.earth-syst>
584 [-dynam.net/8/323/2017/](https://www.earth-syst-dynam.net/8/323/2017/)
- 585 Senior, C. A., & Mitchell, J. F. B. (2000). The time-dependence of climate sensitivity.
586 *Geophysical Research Letters*, *27*(17), 2685–2688. Retrieved from <http://dx.doi>
587 [.org/10.1029/2000GL011373](http://dx.doi.org/10.1029/2000GL011373)
- 588 Shiogama, H., Stone, D., Emori, S., Takahashi, K., Mori, S., Maeda, A., ... Allen, M. R.
589 (2016). Predicting future uncertainty constraints on global warming projections. *Sci-*
590 *entific Reports*, *6*, 18903 EP -.
- 591 Soden, B. J., & Held, I. M. (2006). An Assessment of Climate Feedbacks in Coupled
592 Ocean-Atmosphere Models. *Journal of Climate*, *19*(14), 3354–3360. Retrieved from
593 <http://dx.doi.org/10.1175/JCLI3799.1>
- 594 Song, X., & Zhang, G. J. (2014). Role of Climate Feedback in El Nino-like SST Response to
595 Global Warming. *Journal of Climate*. Retrieved from <http://dx.doi.org/10.1175/>
596 [JCLI-D-14-00072.1](http://dx.doi.org/10.1175/JCLI-D-14-00072.1)
- 597 Stocker, T. F. e. a. (2013). *Climate Change 2013: The Physical Science Basis*. Cambridge
598 University Press, Cambridge, United Kingdom and New York, NY, USA.
- 599 Stouffer, R., & Manabe, S. (2003). Equilibrium response of thermohaline circulation to
600 large changes in atmospheric CO₂ concentration. *Climate Dynamics*, *20*(7-8), 759-
601 773. Retrieved from <http://dx.doi.org/10.1007/s00382-002-0302-4>
- 602 Taylor, K. E., Stouffer, R. J., & Meehl, G. A. (2011). An Overview of CMIP5 and the
603 Experiment Design. *Bulletin of the American Meteorological Society*, *93*(4), 485–498.
604 Retrieved from <http://dx.doi.org/10.1175/BAMS-D-11-00094.1>

- 605 Tian, B. (2015). Spread of model climate sensitivity linked to double-intertropical conver-
 606 gence zone bias. *Geophysical Research Letters*, 42(10), 4133–4141. Retrieved from
 607 <http://dx.doi.org/10.1002/2015GL064119>
- 608 Tierney, J. E., Haywood, A. M., Feng, R., Bhattacharya, T., & Otto-Bliesner, B. L. (2019).
 609 Pliocene Warmth Consistent With Greenhouse Gas Forcing. *Geophysical Research*
 610 *Letters*, 46(15), 9136–9144. Retrieved from [https://agupubs.onlinelibrary.wiley](https://agupubs.onlinelibrary.wiley.com/doi/abs/10.1029/2019GL083802)
 611 [.com/doi/abs/10.1029/2019GL083802](https://agupubs.onlinelibrary.wiley.com/doi/abs/10.1029/2019GL083802)
- 612 Trossman, D. S., Palter, J. B., Merlis, T. M., Huang, Y., & Xia, Y. (2016). Large-scale ocean
 613 circulation-cloud interactions reduce the pace of transient climate change. *Geophysical*
 614 *Research Letters*, 43(8), 3935–3943. Retrieved from [http://dx.doi.org/10.1002/](http://dx.doi.org/10.1002/2016GL067931)
 615 [2016GL067931](http://dx.doi.org/10.1002/2016GL067931)
- 616 Wetherald, R. T., & Manabe, S. (1988). Cloud feedback processes in a general circula-
 617 tion model. *Journal of the Atmospheric Sciences*, 45(8), 1397–1416. Retrieved from
 618 [http://dx.doi.org/10.1175/1520-0469\(1988\)045<1397:CFPIAG>2.0.CO;2](http://dx.doi.org/10.1175/1520-0469(1988)045<1397:CFPIAG>2.0.CO;2)
- 619 Winton, M., Takahashi, K., & Held, I. M. (2010). Importance of Ocean Heat Uptake Efficacy
 620 to Transient Climate Change. *Journal of Climate*, 23(9), 2333–2344. Retrieved from
 621 <http://dx.doi.org/10.1175/2009JCLI3139.1>
- 622 Zhou, C., Zelinka, M. D., Dessler, A. E., & Klein, S. A. (2015). The relationship between
 623 inter-annual and long-term cloud feedbacks. *Geophysical Research Letters*. Retrieved
 624 from <http://dx.doi.org/10.1002/2015GL066698> (2015GL066698)
- 625 Zhou, C., Zelinka, M. D., & Klein, S. A. (2016). Impact of decadal cloud variations on
 626 the Earth’s energy budget. *Nature Geosci*, 9(12), 871–874. Retrieved from [http://](http://dx.doi.org/10.1038/ngeo2828)
 627 dx.doi.org/10.1038/ngeo2828
- 628 Zhou, C., Zelinka, M. D., & Klein, S. A. (2017). Analyzing the dependence of global
 629 cloud feedback on the spatial pattern of sea surface temperature change with a green’s
 630 function approach. *Journal of Advances in Modeling Earth Systems*, 9(5), 2174–2189.
 631 Retrieved from <http://dx.doi.org/10.1002/2017MS001096>